*Journal of Materials & Environmental Sustainability Research* (2025), 5(4): 38-50
p-ISSN: 2811-1338; e-ISSN: 2811-132X
DOI: https://doi.org/10.55455/jmesr.2025.006

Original Research Paper

# A new model for analyzing porosity loss in metallic iron packed-beds for water treatment

**Domga Richard[1]*, Musongo Balike[3], Kom Blaise[2], Inna Samomssa[1], Heukwa-Tefoung Anne[4], Togue Kamga Fulbert[5], Tchatchueng Jean Bosco[1]**

[1] Department of Applied Chemistry, National Advanced School of Agro-Industrial Sciences, University of Ngaoundere, Cameroon
[2] Department of Chemistry, Faculty of Science, University of Ngaoundere, PO Box. 454, Ngaoundere, Cameroon
[3] Department of Chemical Engineering, School of Chemical Engineering and Mineral Industries, University of Ngaoundere, Cameroon
[4] Oakland University William Beaumont School of Medicine, 586 Pioneer Drive Rochester, MI 48309, United States of America
[5] Institute of Fisheries and Aquatic Sciences, University of Douala, Box 2701, Douala, Cameroon

*Corresponding author: domga.richard@yahoo.fr (Domga Richard)

*Received: July 24, 2025; Received in revised form: August 23, 2025; Accepted: September 3, 2025; Published: September 26, 2025*



## Abstract

The objective of this research project is to model all these parameters in the operation of the $Fe^0$ filter in order to better control its design. In this study, we assume that simple cylindrical $Fe^0$ particles corrode uniformly and we use the decrease in radius $\Delta R$ and changes in the height of the iron particles to evaluate the reduction in porosity throughout the system. Parameters such as the volumetric expansion coefficient with oxygen accessibility function, initial radius, primary volume of $Fe^0$, and initial porosity of the system are used to improve the mathematical equation for $Fe^0$ filters. The research indicated that for the variation in oxygen level with $\tau = 0.521$, we obtain a percentage of iron consumption of 59.48% for a volumetric expansion coefficient of $\eta = 2.08$. The same percentage was obtained for a consumption extension $\tau = 1$. Outside the variation of the radius with the height of the particles, the percentage of iron consumed decreases from 99.61 to 83.21. Durable filters must contain an $Fe^0$ content not exceeding 52.10 % (v/v) to comply with the volumetric expansion coefficient of $\eta = 2.08$. The inclusion of this equation in the modelling should improve the permeability loss of the $Fe^0$ filtration system.

**Keywords:** Durable filters, Filtration system, Permeability loss, Reduction in porosity, Volumetric expansion

DOI: 10.55455/jmesr.2025.006

## 1. Introduction

Water pollution is the physical, chemical, biological, or bacteriological degradation of its natural qualities caused by humans and their activities. It disrupts the living conditions of aquatic flora and fauna; it compromises water use and the balance of the natural environment (Ali 2004; Ali, 2012; Chiu, 2013; WHO/UNICEF 2019; UNESCO, 2021; Chen and Wang, 2022 ; Yuan *et al*., 2023; Zhang *et al.,* 2023). According to WHO/UNICEF 2019, there is a

disparity in terms of access to drinking water among the global population, with sub-Saharan Africa being the most affected with 400 million people. Rivers, lakes, and ponds are the direct sources of supply for these populations, particularly in rural areas where there are no centralized drinking water supply systems (WHO/UNICEF, 2025) Water is one of the pillars of sustainable development according to the United Nations' Sustainable Development Goals (SDGs). To achieve the Sustainable Development Goals (SDGs) by 2030, several researchers have studied water treatment methods.

Confronted with this issue, scientists are now exploring various techniques like filtration, adsorption, coagulation, electrocoagulation, membrane filtration, and granular filtration for treating drinking water (Abramian and El-Rassy, 2009; Djonga et *al.*, 2020; Shah *et al.*, 2021 ; Tariq et *al.*, 2021; Bike et *al.*, 2020; Sorayyaei et *al.*, 2021; Danièle et *al.*, 2021 Domga et *al.,* 2022a, Domga et *al.,* 2022b, Arslan-Alaton et Farasat, 2023 ; Senem et *al.*, 2023 ; Domga, 2025). Nevertheless, the majority of these techniques are costly and require high energy consumption. the implementation of other techniques, however, it can be costly (Yanne et *al.*, 2021; Ying et *al.,* 2023; Roberto et *al.,* 2023; Domga, 2025). Oxidation processes are quite costly and have limited implementation.

A straightforward yet efficient method for purifying drinking water is urgently required (Bhaumik et *al.*, 2015). Adapted sand filters containing as much as 50 % metallic iron ($Fe^0$) are highly effective for the decentralized water treatment (Noubactep, 2009a; Noubactep, 2014, Noubactep and Caré, 2011; Noubactep, 2015a; Noubactep, 2015b; Tepong-Tsindé et *al.*, 2015a; Huang et *al.*, 2021; Ogata et *al.*, 2021). The technology is perfect for underdeveloped rural areas. $Fe^0$/sand filters can effectively remove various chemical contaminants (organic and inorganic) as well as pathogens (bacteria and viruses) (Noubactep, 2009a; Henderson and Demond 2007; Guan et *al.*, 2015; Bojic et *al.,* 2001; Bojic et *al.*, 2004; You et *al.*, 2014; Ndé-Tchoupé et *al.*, 2020; Huang et *al.*, 2021; Yang et *al.*, 2020; Njaramba, et *al.*, 2021; Amoako-Nimako et *al.*, 2021; Ogata et *al.*, 2021; Anderson-Coughlin et *al.*, 2021). $Fe^0$/sand filters are relatively efficient, low-cost, plentiful, eco-friendly, and simple to set up. They can also be configured for gravity flow without needing power. Iron oxide and silica are plentiful and easily found in the surroundings. The $Fe^0$ / sand filter can be conveniently created for drinking water supply in households and small communities (Nitzsche et *al.*, 2015; Tepong-Tsindé et *al.*, 2015a; Rahman et *al.*, 2013; Togué-Kamga et *al.*, 2012; Yang et *al.*, 2020; Gong et *al.*, 2021; Huang et *al.*, 2021; Ogata et *al.*, 2021; Sun et *al.*, 2021). Several studies have been conducted to reassess the appropriateness of metallic iron ($Fe^0$) as a filter material for providing decentralized drinking water. The research conducted by Miyajima, 2012; Rahman et *al.*, 2013, Btatkeu et *al.*, 2014a and Tepong-Tsinde et *al.*, 2015b established the best volumetric ratio of $Fe^0$/sand as 25/75. The incorporation of composite materials based on $Fe^0$ nanoparticles, bimetallic cations, metal oxides in activated carbon, graphene, biochar have been used as composite material for the removal of organic and inorganic compounds (Bafghi et *al.*, 2008, Noubactep and Caré, 2011; Btatkeu et *al.*, 2014b; Chen et *al.*, 2014; Hu et *al.,* 2020; Du et *al.*, 2020 ; Xiao et *al.,* 2020 ; Cao et *al.*, 2021; Chen et *al.*, 2022; Kaur et *al.*, 2023; Dong et *al.*, 2023; Huang et *al.*, 2023; Gao et *al.*, 2023; He et *al.*, 2024; Li et *al.*, 2024; Dong et *al.*, 2025).

Moreover, in the reactive zones, little attention has been devoted to the size and shape of the metallic iron particles (spherical or cylindrical), but these two parameters influence not only the porosity and the consumption of the iron but also the settlement of the columns. Hussam 2009, Hussam and Munir 2007 used composite iron matrix and cylindrical iron particles for the total elimination of arsenic. While Noubactep and Caré, 2010 utilized spherical and cylindrical iron particles, Rahman et *al.*, 2013 opted for the same approach to model hydraulic conductivity. The research conducted by Btatkeu et *al* in 2013 explored the reactivity of various iron types for $Fe^0$/sand filter applications. There has been limited research on the design principles for $Fe^0$ filters. From 2008 onwards, studies on $Fe^0$ filters have shown that despite being effective, they lack durability (Noubactep and Caré, 2011; Caré et *al.*, 2008). Designing and optimizing a filtration system is challenging because of the constantly changing water conditions and mechanisms within the filter (Cookson, 1970; You et *al.*, 2014). There is still ongoing research on the design of traditional filters, as stated by You et *al* in 2014 and Zielina in 2011. The results of the work by Yang et *al* in 2021 showed that the model's assumptions concerning iron corrosion rates depend on first-order iron surface kinetics and can only be valid when no iron surface passivation is taken into account. Domga et *al* in 2015 and Domga et *al* in 2017 introduced a general formula showing the radius difference of a spherical and cylindrical substance ($X = R_0-R$) based on: (i) initial particle size ($R_0$), (ii) $Fe^0$ depletion quantity ($V_{oxide}$), initial $Fe^0$ amount ($V_{ZVI}$), and (iii) dissolved oxygen availability ($\eta$ value). The work of Domga et *al* in 2015 made it possible to model these parameters in the operation of the $Fe^0$ filter for the better control of its design for spherical-shaped particles. The work of Domga et *al* in 2017 on cylindrical iron particles enabled us to establish a

mathematical model taking into account particle radius, oxygen level and the volumetric proportion of $Fe^0$. This modeling work, carried out on cylindrical iron particles, did not take into account the variation in the height of $Fe^0$ particles with the variation in particle size radius. This parameter influences the production of iron corrosion products in $Fe^0$ filters. This parameter influences the production of iron corrosion products in $Fe^0$ filters. This research work aims at recapitulating and complementing more recent works and consolidating/providing a scientific base for the designation of a cylindrically-shaped $Fe^0$ filter while taking into account the loss of iron radius consumed with a variation in particle height. It shows how to properly characterize.

## 2. Materials and Methods

Calculation of $X=R_0-R$; $Y=h_0-h$

The approach utilized in this section includes determining the decrease in radius ($X=R_0-R$) and height ($Y=h_0-h$) of an individual cylindrical $Fe^0$ grain and studying their effects on reducing porosity.

### 2.1 Evaluation of $X = R_0 - R$; $Y = h_0 - h$

In this analysis, we will examine cylindrical particles that have the same radius R0 and height. The volume of these particles ($V_{part}$) is given by $V_{part} = Sh_0 = h_0\pi R_o^2$, where $h_0$ is the height of particles. The number of particle ($N_{ZVI}$) filling a volume $V_{ZVI}$ is $N_{ZVI}=V_{ZVI}/V_{part}$. The mass of a particle ($m_{part}$) is expressed by $m_{part} = \rho V_{part}$, where ϱ is the specific weight of the material. At the initial time ($t_0$=0), the mass of a particle is $m_{opart} = \pi\rho h_0 R_o^2$ and it volume at time $t > t_0$ is $m_{part} = \pi\rho h R^2$. The mass loss correspondent can be determining as:

$\delta_m = m_{opart} - m_{part} = \rho h_0 \pi R_o^2 - h\rho\pi R^2$.

Replacing $R = R_0 - X$ and $h = h_0 - Y$

$\delta_m = m_{opart} - m_{part} = \pi\rho(h_0 R_o^2 - hR^2)$

Substituting R and h into the previous equation $\delta_m$ reads as:

$$\boldsymbol{\delta_m} = -\pi\rho[X^2(h_0 - Y) - 2R_0X(h_0 - Y) - YR_0^2] \quad (1)$$

For a system containing $N_{ZVI}$ particle, the mass loss for the whole system, containing $N_{ZVI}$ particles is given by Eq. (2):

$$\boldsymbol{\Delta_m} = -\sum_1^{NZVI} \pi\rho[X^2(h_0 - Y) - 2R_0X(h_0 - Y) - YR_0^2] \quad (2)$$

$V_{ZVI}$, $R_0$ and $h_0$ are are the variables that serve as parameters in this equation. X=0, Y=0, are associated to the initial particle as R= $R_0$, h= $h_0$. X = $R_0$, Y = $h_0$ are associated to $Fe^0$ total depletion as R= 0, h= 0. The volume of oxide ($V_{ox}$) produced and the initial pore volume ($V_{pore}$) of the filter parameters are involve in $Fe^0$ depletion. If $V^{\infty}_{ox} <= V_{pore}$, $Fe^0$ complete depletion can be achieved else $Fe^0$ depletion should be partial since a fraction of the initial quantity of $Fe^0$ will not react because space is needed for volumetric expansion. This surplus $Fe^0$ demonstrates a pure material wastage (Togue-Kamga et *al*., 2011; Antia et *al*., 2014). In the case that ($V^{\infty}_{ox} = V_{pore}$) associates to entire pore fouling by iron corrosion products, $R_0$ is equal to X and $h_0$ is equal to Y. Hence, the discussion about system clogging should be appropriate with Eq. (2) only if $R_0$ is larger than X ($R_0 > X$) and $h_0$ is larger than h ($h_0 > Y$).

$$\Delta_m = \rho \times \Delta V_{ZVI} = \rho \times V_{oxyde}/(\eta - 1) \quad (3)$$

$$\Delta V_{ZVI} = V_{oxyde}/(\eta - 1) \quad (4)$$

Rahman et *al*., 2013 has established the relationship (Eq. (4)) between $\Delta V_{ZVI}$ and $V_{oxyde}$. Rearranging Eq. (2), Eq. (3) and Eq. (4) yields the following second degree equation in X (Eq. (5)):

$$[X^2(h_0 - Y) - 2R_0X(h_0 - Y) - YR_0^2] + \frac{V_{oxyde}}{V_{ZVI}} \times \frac{h_0 R_0^2}{(\eta - 1)} = 0 \quad (5)$$

Eq. (5) is suitable to discuss system clogging following $Fe^0$ depletion. This equation shows that the degree of radius reduction of a $Fe^0$ particle are determined by the following factors: the initial dimension of the particles ($R_0$, $h_0$), the volume of oxide produce ($V_{oxide}$), the initial volume of $Fe^0$ ($V_{Fe^0}$), and the accessibility of dissolved oxygen (η value). As the intrinsic reactivity of $Fe^0$ material is not developed in Eq. (5), this equation should be

frequently used to design experiment with $Fe^0$. Eq. (5) should be also regularly used to assess the results with different materials under comparable conditions. Ideally, such a systematic research should be performed under unified experimental conditions (standard protocols). To extend the life service of systems, non-expansive materials (e.g. sand) should be admixed to $Fe^0$. In this case, Eq. (5) has to heed the case of mixture systems. The volumetric ratio of $Fe^0$ in the solid mixture, $V_{ZVI} = \tau_{ZVI}\ V_{solid}$ and Eq. (5) is rearranged as:

$$X^2(h_0 - Y) - 2R_0X(h_0 - Y) - YR_0^2 + \left(\frac{V_{oxyde}}{V_{solide}}\right) \times \frac{h_0R_0^2}{[\tau_{ZVI} \times (\eta - 1)]} = 0 \qquad (6)$$

## 2.2 Expression of the extent of $Fe^0$ depletion

Eq. (6) is solve analytically to find the values of X as function of Y. Non porous materials are considered. Since $0 < X < R_0$ and $0 < Y < h_0$, Eq. (6) include two solutions but only one solution is physically acceptable. To solve Eq. (6) a theoretical system with a total volume of 1000 mL and a porosity of 36% containing $Fe^0$ particles with equal radius of 1.0 mm and equal height of 2.0 mm is assumed. In such a system the initial $V_{Fe^0} = 640$ mL yielding an initial pore volume $V_{pore} = 360$ mL. The volumetric expansion coefficient η values (2.08, 3.75, 4.20 and 6.40) used are provided by Caré et *al*., 2008.

The proportion law is used to determine the residual $Fe^0$ mass associated to X and Y

value as:

$$m = m_0 \frac{(ho-y)(Ro-x)^2}{R_0^2 h_0} \qquad (7)$$

The weight percent of $Fe^0$ corroded and the percent of remaining $Fe^0$ are wrote Eq (8) and Eq (9) as:

$$P_R = 100\,(m/m_0) = 100\ \frac{(ho-y)(Ro-x)^2}{R_0^2 h_0} \qquad (8)$$

$$P_C = 100 - P_R \qquad (9)$$

$P_R$ and $P_C$ are respectively the residual and the consumed mass percent of $Fe^0$.

Similarly, the volumetric percent of $Fe^0$ corroded is wrote Eq. (10) as:

$$V = V_0 \frac{(ho-y)(Ro-x)^2}{R_0^2 h_0} \qquad (10)$$

# 3. Results and Discussion

## 3.1 Dissolved oxygen level and porosity loss

**Figure 1** summarizes the extent for $Fe^0$ consumption as function of the volumetric expansion coefficient of iron corrosion (η values). Working conditions: Vsystem = 1.0 L, initial porosity ($\Phi_0$) = 36%, $R_0$ = 1.0 mm, $h_0$ =2 mm. Uniform corrosion is assumed and material is supposed to be compact cylindrical particles. The initial systems porosity $\Phi_0$= 36%. In real systems, irregularly shaped particles are fundamentally more porous ($\Phi_0 > 36\%$) (Kamolpornwijit and Liang, 2006; Jeen et *al*., 2008).

Dissolved oxygen is probably the most corrosive factor of iron under environmental conditions (Mackenzie et *al*., 1999; Kamolpornwijit et *al*., 2003; caré et *al*., 2008; Bartzas and Komnitsas, 2010; Caré et *al*., 2013). Resulting from the products of corrosion, it is a mixture of hydrated iron and crystallized oxides, generally called rust. This study deals with the relationship between oxygen availability and porosity/permeability loss. The presentation in this section is limited to showing the relationship between $O_2$ availability and the nature of the products of iron corrosion. **Figure 1** respectively give the results of the variation of the radius as a function of the height of the cylindrical particles for four values of the volumetric expansion coefficient η. The selected values represent the variant operating conditions of the anoxic (absence of $O_2$) conditions (η = 2.08-$Fe_3O_4$) under oxic (presence of $O_2$) conditions (η = 6.40 - $Fe(OH)_3$) .$6H_2O$) (Rahman et *al*., 2013). It is evident from **Figure 1** that only the systems studied under anoxic conditions could reach a value of X/Ro close to 94.94% and Y/ho close to 95.5%, corresponding approximately to 100% of the initial amount of $Fe^0$ consumed. The amount of $Fe^0$ consumed in all other systems is less than 100%. Therefore, a fraction of the initial quantity of $Fe^0$ will not react. For the systems

studied under oxic conditions the value of X/Ro is less than 10.33% and Y/ho less than 19.5%, corresponding approximately to 20% of the initial amount of $Fe^0$ consumed. $Fe^0$ depletion should be partial because space is needed for volumetric expansion. **Figure 1** shows that the amount of $Fe^0$ consumed increases in all systems when volumetric expansion coefficient decrease (i.e avaibility of $O_2$ is reduced). Previous results show that all $Fe^0$-durable filters are those containing spherical particles (Rahman et *al.,* 2013; Domga et *al.,* 2015b) and operate under anoxic conditions. This study shows that all $Fe^0$- lasting filters are those operating under anoxic environmental conditions. This knowledge demonstrates that dissolved oxygen is the most corrosive factor of iron under environmental conditions (Caré et *al.*, 2013). The oxidation of iron in the $Fe^0$ system strongly influences the permeability loss process and therefore its durability (Mackenzie et *al.,* 1999).

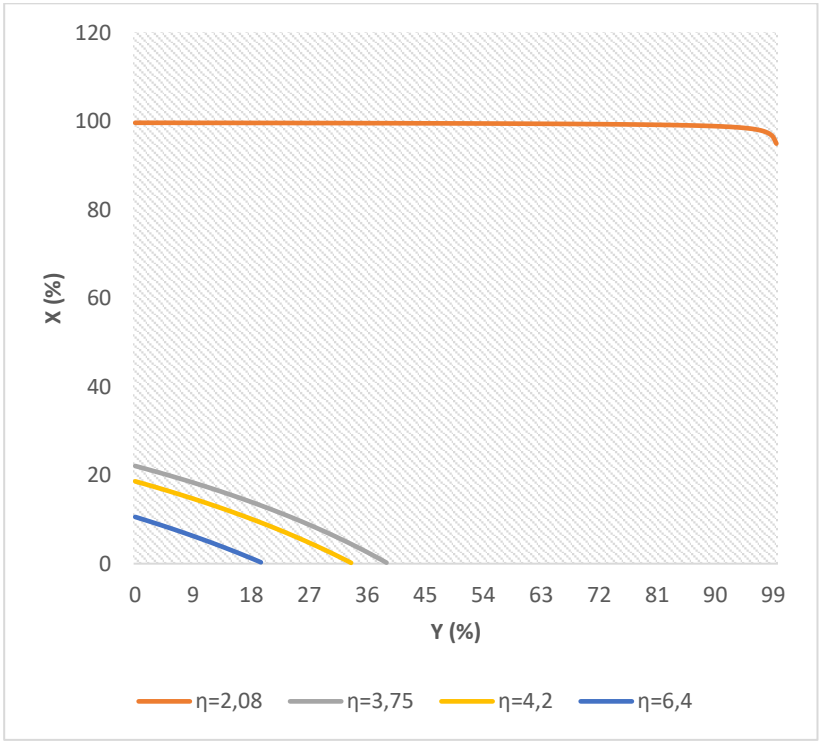


**Figure 1**. Effect of the volumetric expansion coefficient of iron corrosion (η values) on the $Fe^0$ consumption extension (τ=0.521).

**Table 1.** Effect of the volumetric expansion coefficient of iron corrosion (η values) on the $Fe^0$ consumption extension (τ=0.521).

| **η** | **2.08** | **3.75** | **4.20** | **6.40** |
|---|---|---|---|---|
| **Oxide** | **$Fe_3O_4$** | **$Fe(OH)_2$** | **$Fe(OH)_3$** | **$Fe(OH)_3.6H_2O$** |
| **X (mm)** | 0.26 | nd | nd | nd |
| **Y (mm)** | 0.52 | nd | nd | nd |
| **R (mm)** | 0.74 | 1.00 | 1.00 | 1.00 |
| **h (mm)** | 1.48 | 2.00 | 2.00 | 2.00 |
| **$P_R$ (%)** | 40.52 | 100.00 | 100.00 | 100.00 |
| **$P_C$ (%)** | 59.48 | 0.00 | 0.00 | 0.00 |

**Table 1** shows the variation in oxygen level, taking into account the variation in radius with the height of the cylindrical iron particles in the system. From this table, it emerges that: the variation of η for values ranging from 2.08 to 6.40, is only favorable under anoxic conditions (η = 2.08-$Fe_3O_4$) with a percentage of iron consumed of 59.48% and 0.00% under oxic conditions (η = 6.40 - Fe $(OH)_3$. Research by Domga et *al* in 2017 showed that for a variation in cylindrical particle radius at constant height the percentage of iron consumed is 51% under anoxic conditions (η= 2.08-$Fe_3O_4$) and 9.75% under oxic conditions (η= 6.40 - $Fe(OH)_3$). The percentage of iron

consumption under anoxic conditions (η = 2.08-$Fe_3O_4$) is greater than under oxic conditions, this result confirms the work of Domga et *al* in 2015 carried out on the variation in the radius of spherical iron particles. The variation in radius with the variation in height of cylindrical iron particles is a parameter to be taken into account when assessing the percentage of iron consumed in the system.

### 3.2 Effect of the volumetric fraction of $Fe^0$ in the material mixture

Eq. (6) is solve for four different values of $\tau_{Fe^0}$ under anoxic conditions (η = 2.08). The results are summarized in **Figure 2**. This figure shows the variation percentage of X/Ro as a function of Y/ho for different values of $\tau_{Fe^0}$. Four values of $\tau_{ZVI}$ under anoxic environment are used to solve graphically Eq.(6) and therefore determine $Fe^0$ depletion extension as function of its initial volumetric fraction in the system. It is shown from **Figure 2** that all the different values of $\tau_{ZIV}$ are solutions of the equation.

This system studied under anoxic conditions reach a value of X/Ro close to 94.94 % and Y/ho close to 95.5 %, corresponding approximately to 100% of the initial amount of $Fe^0$ consumed for $Fe^0$-filters containing 52.084% $Fe^0$ (v/v) of cylindrical particles. The amount of $Fe^0$ consumed in all other systems is less than 100%. For a systems containing 100 % $Fe^0$ (v/v) of cylindrical particles under anoxic conditions, X/Ro reach a value close to 30.60 % and Y/ho close to 52 %, corresponding approximately to 52% of the initial amount of $Fe^0$ consumed. In this case these filters should be effective but not durable. **Figure 2** shows that the amount of $Fe^0$ consumed decreases in $Fe^0$ systems when volumetric fraction increases. This study shows that all $Fe^0$- lasting filters are those inclosing 52,084 % $Fe^0$ (v/v) for cylindrical particles and operate under anoxic conditions.

Previous work shows that the system consists of spherical particles with the value $\tau_{ZVI} > 0.5209$ (52.0 % $Fe^0$ (v/v)), is clogged before the complete consumption of $Fe^0$, while other systems with $\tau_{ZVI}$ values less than 0.5209 do not clog (Domga et *al*., 2015b). In these systems, the complete consumption of $Fe^0$ is likely to occur during the remediation time, depending on the intrinsic reactivity of the material used and the impact of the environmental conditions of this.

Despite documentation of the loss of hydraulic conductivity of $Fe^0$ filters for contaminant-free systems (Luo et *al*., 2013), 100 % $Fe^0$ filters are not durable as well as filters using cylindrical particles. In such system particle height varies with the radius regardless of the value of $\tau_{ZVI}$ used. Permeability loss of $Fe^0$ filters for contaminant free systems has been documented (Henderson and Demond, 2013). Although it is not necessarily due to complete pore filling, but mostly due to reduced interconnectivity of pores, these results critically question the rationale for building $Fe^0$ PRBs, incorporating $Fe^0$ filters containing zones with 100 % $Fe^0$.

**Table 2.** Effect of volumetric proportion of iron ($\tau_{ZVI}$) in the solid fraction on $Fe^0$ depletion (η= 2.08)

| **τ** | 1 | 0.52 | 0.35 | 0.20 | 0.10 |
|---|---|---|---|---|---|
| **X (mm)** | 0.26 | 0.11 | 0.07 | 0.04 | 0.02 |
| **Y (mm)** | 0.52 | 0.22 | 0.14 | 0.08 | 0.04 |
| **R (mm)** | 0.74 | 0.89 | 0.93 | 0.96 | 0.98 |
| **h (mm)** | 1.48 | 1.78 | 1.86 | 1.92 | 1.96 |
| **$P_R$ (%)** | 40.52 | 70.50 | 80.44 | 88.47 | 94.12 |
| **$P_C$ (%)** | 59.48 | 29.50 | 19.56 | 11.53 | 5.88 |

**Table 2** shows the variation in volumetric fraction, taking into account the variation in radius with height of the cylindrical iron particles in the system. The variation in rate for values ranging from 1 to 0.1 results in a decrease in the percentage of iron consumed in the system from 59.48% to 5.88%, when taking into account the variation in radius with particle height. For a constant particle size height, the percentage of iron consumed varies from 51 to 100% for rate values ranging from 1 to 0.1. The variation of radius with height influences the percentage of iron consumed when rates are taken into account in the system.

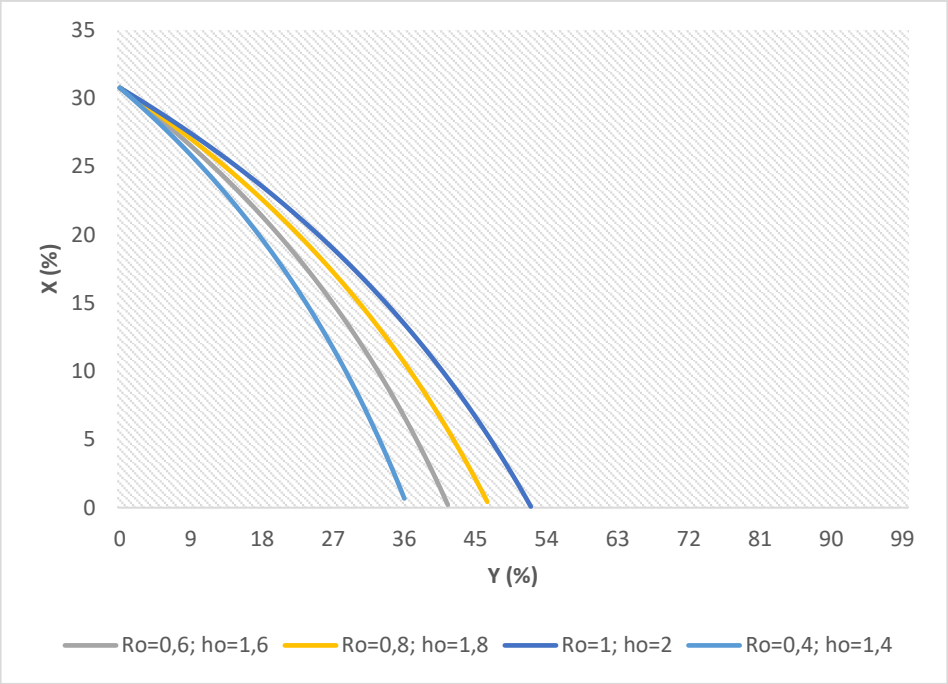


**Figure 2.** Effect of volumetric proportion of iron ($\tau_{ZVI}$) in the solid fraction on $Fe^0$ depletion ($\eta$= 2.08).

### 3.3 Impact of the initial $Fe^0$ particle size

Beside $\tau_{ZVI}$ and $\eta$ values, an essential parameter for the effectiveness of a $Fe^0$ filter is the range of the particles used ($R_0$ and $h_0$). **Figure 3** summarizes the results of the solution Eq. 6 as a function of X and Y for four different values of $R_0$ and $h_0$. For this work, the uniform corrosion is supposed and we set the volume of the system (1l), the initial porosity ($\Phi_0$ = 36%), the volumetric expansion ($\eta$ = 2.08) and the volumetric proportion ($\tau_{ZVI}$ = 1). From **Figure 3**, it is obvious that a systems containing cylindrical particles ($R_0$ =1mm and $h_0$ = 2 mm) under anoxic conditions, X/Ro and Y/ho reach values close to 30.42 % and 52 % respectively. While a systems containing cylindrical particles ($R_0$ = 0.8 mm and $h_0$ =1.8 mm) in the same environment conditions, X/Ro and Y/ho reach values close to 30.42 % and 36 % respectively, corresponding in both cases approximately to 52 % of the initial amount of $Fe^0$ consumed. This study shows that in all $Fe^0$-filters containing cylindrical particles and operate under anoxic conditions, the amount of $Fe^0$ consumed increases with the initial $Fe^0$ particle size. However, the magnitude of $Fe^0$ consumption for different $Fe^0$ particles size is less than 100 % ($P_C$ < 100 %) in the system during the variation of cylindrical particle radius with height. Nevertheless, it should be kept in mind that the larger particles are of similar low reactivity. This was the reason for the introduction of nanoparticles from $Fe^0$ materials (Zhang et *al*., 1998).

**Table 3.** Effect of $Fe^0$ initial particle size ($R_0$, $h_0$) on the $Fe^0$ consumption extension

| $R_O$ (mm) | $h_O$ (mm) | X (mm) | Y (mm) | R (mm) | h (mm) | $P_R$ (%) | $P_C$ (%) |
|---|---|---|---|---|---|---|---|
| **1.00** | 2 | 0 .305 | 0.520 | 0.095 | 1.040 | 0.383 | 99.617 |
| **0.80** | 1.8 | 0.305 | 0.465 | 0.295 | 1.185 | 4.457 | 95.543 |
| **0.60** | 1.6 | 0.305 | 0.415 | 0.495 | 1.335 | 10.528 | 89.472 |
| **0.40** | 1.4 | 0.305 | 0.360 | 0.695 | 1.480 | 16.785 | 83.215 |

**Table 3** shows the variation in particle size, taking into account the variation in radius with the height of the cylindrical iron particles in the system. Y values decrease with particle height, R decreases with increasing particle height for constant X values. The percentage of residual iron increases with decreasing particle height from 0.383 to 16.785% for initial heights ranging from 2.00 to 1.40 mm and initial radii from 1.00 to 0.40 mm, while the percentage of iron consumed decreases from 99.617 to 83.215% with increasing particle heights and radii. The

variation in radius with height influences the percentage of iron consumed when the variation in particle height in the system is taken into account.

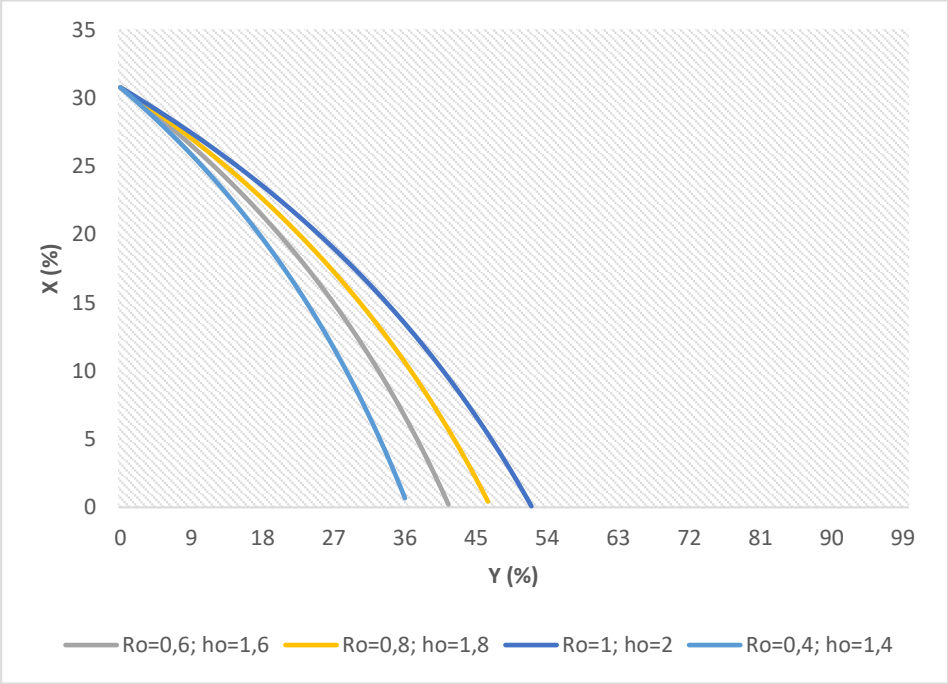


**Figure 3**. Effect of $Fe^0$ initial particle size ($R_0$, $h_0$) on the $Fe^0$ consumption extension

## 4. Conclusion

In this work, a new universal equation of the cylindrical particles of the $Fe^0$ filters is developed, control parameters are X (the initial radius $R_0$), Y (the initial height of $Fe^0$ particles), the initial porosity of the filter, the coefficient of volumetric expansion (availability of $O_2$) and the volumetric fraction of $Fe^0$ in the material mixture. These various relevant parameters analysed have demonstrated that the oxidation of iron in the $Fe^0$ system strongly influences the permeability loss process and therefore its durability. The results showed that the variation of the cylindrical iron particles radius and height do not necessary causes a higher consumption of the iron under the anoxic conditions. However, the change of the volumetric proportion and the volumetric fraction of $Fe^0$ in the material mixture strongly initiate a higher consumption of the iron under the anoxic conditions. Modelling the evolution of hydraulic conductivity in modified $Fe^0$ filters should be improved by using the ray and height loss expression of each reactive particle provided in this work.

### Conflict of Interest

The authors declare no conflict of interest.

### Author contributions

For this research paper, Conceptualization, Domga Richard; methodology, Kom Blaise; software, Musongo Balike; validation, Togue Kamga Fulbert and Tchatchueng Jean Bosco; formal analysis, Inna Samomssa; investigation, Inna Samomssa; resources, Domga Richard; data curation, Togue Kamga Fulbert; writing—original draft preparation, Domga Richard; writing—review and editing, Musongo Balike; visualization, Togue Kamga Fulbert; supervision, Tchatchueng Jean Bosco; project administration, Togue Kamga Fulbert. All authors have read and agreed to the published version of the manuscript.

**Declaration**

This article is a continuation of research by Domga et *al*., 2017.
Richard Domga**,** Togue-Kamga F., Tchatchueng J B. **(2017).** Mathematic analysis of porosity loss in granular metallic iron ($Fe^0$) water filter. *International Journal of Emerging Engineering Research and Technology*, 5(11), 28-35.

**References**

Abramian, L. & El-Rassy, H. (2009). Adsorption of kinetics and thermodynamics of azo-dye Orange II onto highly porous titania aerogel. Chemical Engineering Journal, 150:403–410.

Ali, I. (2014). Water treatment by adsorption columns: Evaluation at ground level. Separation and Purification Reviews. 43(3):175–205.

Ali, I. (2012). New generation of adsorbents for water treatment. Chemical Reviews, 112:5073-5091.

Amoako-Nimako, G.K., Yang, X. & Chen, F. (2021). Denitrification using permeable reactive barriers with organic substrate or zero-valent iron fillers: Controlling mechanisms, challenges, and future perspectives. Environmental Science Pollution Research, 28: 21045–21064.

Anderson-Coughlin, B.L., Litt, P.K., Kim, S., Craighead, S., Kelly, A.J., Chiu, P., Sharma, M. & Kniel, K.E. (2021). Zero-valent iron filtration reduces microbial contaminants in irrigation water and transfer to raw agricultural commodities. Microorganisms, 9, 2009.

Antia D.D.J., Kharisov, B.I., Kharissova, O.V, & Rasika Dias, H.V. (2014). Groundwater water remediation by static diffusion using nano-zero valent metals ($Fe^0$, $Cu^0$, $Al^0$), n-$FeH^{n+}$, n-$Fe(OH)_x$, n-FeOOH, n-Fe-$[O_xH_y]^{(n+/-)}$, In "Nanomaterials for Environmental Protection"1–25, doi: 10.1002/9781118845530.ch1.

Arslan-Alaton, I. & Farasat, S. (2023). The Use of Peroxides as Green Oxidants for Color Removal from Textile Industry Wastewater. Advance research in textile engineering, 8(1); 1078.

Bafghi, M.S., Zakeri, A., Ghasemi, Z. & Adeli, M, (2008). Reductive dissolution of manganese ore in sulfuric acid in the presence of iron metal. Hydrometallurgy, 90:207–212.

Bartzas, G. & Komnitsas, K. (2010). Solid phase studies and geochemical modelling of low Cost permeable reactive barriers. Journal of Hazardous Materials, 183:301–308.

Bhaumik, M., Noubactep, C., Gupta, V.K., McCrindle, R.I. & Maity (2015). A Polyaniline/$Fe^0$ Composite nanofiber: An excellent adsorbent for the removal of arsenic from aqueous Solutions. Chemical Engineering Journal, 271 :135–146.

Bike-Mbah, J.B., Benessoubo, K., Eko, M., Tekoumbo, T., Elimbi, A. & Kamga, R. (2020). Adsorption mechanisms of pigments and free fatty acids in the discoloration of shea butter and palm oil by an acid- activated Cameroonian smectite. Scientific African, 9: e00498.

Bojic, A., Purenovic, M., Kocic, B., Perovic, J., Ursic-Jankovic, J, & Bojic, D. (2001). The inactivation of Escherichia coli by microalloyed aluminium based composite Facta Universitatis-series: Physics, Chemistry and Technology, 2:115–124.

Bojic, A., Purenovic, M. & Bojic, D. (2004). Removal of Chromium (VI) from Water by Micro Alloyed Aluminium Based Composite in Flow Conditions. Water SA, 30 :353- 357.

Btatkeu, B.D., Miyajima, K., Noubactep, C. & Caré, S. (2013). Testing the suitability of metallic iron for environmental remediation: Discoloration of methylene blue in column studies. Chemical Engineering Journal, 215–216:959–968.

Btatkeu, B.D., Olvera-Vargas, H., Tchatchueng, J.B., Noubactep, C. & Caré, S. (2014a). Determining the optimum $Fe^0$ ratio for sustainable granular $Fe^0$/sand water filters. Chemical Engineering Journal, 247:265–274.

Btatkeu, B.D., Olvera-Vargas, H., Tchatchueng, J.B., Noubactep, C. & Caré, S. (2014b). Characterizing the impact of $MnO_2$ on the efficiency of $Fe^0$-based filtration systems. Chemical Engineering Journal, 250:416–422.

Cao, V., Alyoussef, G., Gatcha-Bandjun, N., Gwenzi, W. & Noubactep, C. (2021). The suitability of methylene blue discoloration (MB method) to investigate the $Fe^0/MnO_2$ system. Processes, 9, 548.

Caré, S., Crane, R., Calabro, P. S., Ghauch, A., Temgoua, E. & Noubactep, C. (2013). Modeling the Permeability Loss of Metallic Iron Water Filtration Systems. Clean-Soil, Air, Water, 41: 275–282.

Caré, S., Nguyen, Q.T., L'Hostis, V. & Berthaud, Y. (2008). Mechanical properties of the rust layer induced by impressed current method in reinforced mortar. Cement and Concrete Research, 38:1079–1091.

Chiu, P, C. (2013). Applications of zero-valent iron (ZVI) and nanoscale ZVI to municipal and decentralized drinking water systems–a review, Novel solutions to water pollution ACS Symposium Series, Vol. 1123.

Chen, H., & Wang, S. (2022). "Accelerated Transition between dry and wet Periods in a Warming Climate." Geophysical Research Letters, 49: e2022GL099766.

Chen, W.F., Pan, L., Chen, L.F., Wang, Q. & Yan, C.C. (2014). Dechlorination of hexachlorobenzene by nano zero-valent iron /activated carbon composite: iron loading, kinetics and pathway. RSC Advances, 4: 46689–46696.

Chen, Y., Zhang, J.W. & Xu, H. (2022). Exploration of the degradation mechanism of ciprofloxacin in water by nano zero-valent iron combined with activated carbon and nickel. Journal of Molecular Liquids, 345:118212

Cookson, J.T. (1970). Removal of submicron particles in packed beds. Environmental Sciences and Technology, (4): 128–134.

Danièle, B. K., Baptiste, B. M. J., Richard, K., & Dinica, R. (2021). Valorization of mango peels as low-cost biosorbent in methylene blue adsorption: kinetic and equilibrium study. Journal of Materials Science and Engineering A, 11(2): 40-47.

Djonga, W. G., Noubissie, E., Noumi, G. B., (2020). Influence of time and oxygenation on the degradation of organic matter, nitrogen and phosphates during the biological treatment of slaughterhouse effluent. Case Studies in Chemical and Environmental Engineering, 2: 100048.

Domga. R., Massai, H., Tcheka, C., Tchatchueng, J.B., Arbam, T., Kobbe, D. N. & Dangwang. D. (2015a). Batch Equilibrium, Kinetic and Thermodynamic Studies on the Adsorption of Methylene Blue in Aqueous Solution onto Activated Carbon Prepared from Bos Indicus Gudali Bones. Chemistry Journal, 1(6):172-181.

Domga. R., Togue-Kamga. F., Noubactep, C. & Tchatchueng, J.B. (2015b). Discussing porosity loss of $Fe^0$ packed water filters at ground level. Chemical Engineering Journal, 263:127-134.

Domga ,R., Togue-Kamga, F. & Tchatchueng, J.B. (2017). Mathematic analysis of porosity loss in granular metallic iron ($Fe^0$) water filter. International Journal of Emerging Engineering Research and Technology, 5(11): 28-35.

Domga, R., Musongo, B., Ze, W., Kolwa, E. D., Domga, W. B., Motue, W. L. C., Arbam, T., Anrakang, B. P. & Tchatchueng, J.B. (2022). Preparation and characterization of an activated carbon from the bones of *Gudali (BosIndicus)* cattle from Adamawa, Global Scientific Journal, 10(1): 895- 913.

Domga, R., Abia, D., Mouthe, A. G. A., Musongo, B., Domga, W. B. & Tchatchueng, J. B. (2022). Optimization of Methylene Blue Adsorption on to activated carbon from Bos Indicus Gudali bones using a Box Behnken Experimental Design, American Journal of Chemistry, 12(1): 1- 9.

Domga, R. (2025). Removal of the methylene blue using activated charcoal derived from the pyrolisis of Gudali (Bos Indicus) bones Generis Publishing 56p.

Dong, J.T., Ji, S.N., Zhang, Y., Ji, M.X., Wang, B., Li, Y.J., Chen, Z.G., Xia, J.X. & Li, H.M. (2023). Construction of Z-scheme $MnO_2$/BiOBr heterojunction for photocatalytic ciprofloxacin removal and $CO_2$ reduction. Acta Physico- Chimica Sinica, 39:2212011.

Dong, K., Zhang, X., Li, D., Xiong, K., Ren, L., Sun, M. & Lv, Z. (2025). Rapid removal of 2,4-DCP by activated carbon loaded nano-zero valence iron immobilized microorganisms. International Biodeterioration & Biodegradation, 201 : 106071.

Du, M., Zhang, Y., Zeng, X., Kuang, H. & Huang, S. (2020). Enhancement of ballmiling on pyrite/zero-valent iron for arsenic removal in water: A mechanistic study. Chemosphere, 249: 126130.

Gao, F.L., Lyu, H., Ahmad, S., Xu, S.Y. & Tang, J.C. (2023). Enhanced reductive degradation of tetrabromo bisphenol A by biochar supported sulfidated nanoscale zero-valent iron: selectivity and core reactivity. Applied Catalysis B Environment and Energy, 324:122246

Gong, L., Qiu, X., Cheng, D., Hu, Y., Zhang, Z., Yuan, Q., Yang, D., Liu, C., Liang, L. & He, F. (2021). Coincorporation of N and S into zero-valent iron to enhance TCE dechlorination: Kinetics, electron efficiency, and dechlorination capacity. Environment Science and Technology, 55: 16088–16098.

Guan, X., Sun, Y., Qin, H., Li, J., Lo, I. M. C., He, D. & Dong, H. (2015). The limitations of applying zerovalent iron technology in contaminants sequestration and the corresponding counter measures: The development in zero-valent iron technology in the last two decades (1994–2014). Water Research, 75: 224–248.

He, L.Z., Wang, S.Q., Luo, F., Liu, Z., Wu, Y., Yang, Y.D. & Chen, Z.Q. (2024). Unravelling the bifunctional role of biochar in promoting nZVI/Ni towards complete dechlorination of trichloroethylene: not only a carbonaceous support. Chemical Engineering Journal. 481:148634

Henderson, A.D. & Demond, A. H. (2007). Long-term performance of zerovalent iron permeable reactive barriers: a critical review. Environment Engineering Science, 24:401–423.

Henderson, A.D. & Demond, A. H. (2013). Permeability of iron sulfide (FeS)-based materials for groundwater remediation. Water Research, 47:1267–1276.

Huang, Z., Cao, V., Nya, E.L., Gwenzi, W. & Noubactep, C. (2021). Kanchan arsenic filters and the future of Fe0-based filtration systems for single household drinking water supply. Processes, 9, 58.

Huang, X.Z., Zhang, Y.X., Zhang, D.S., Ding, W.H. & Hu, X.X. (2023). Reduced graphene oxide supported Fe/Ni bimetallic nanoparticles for the rapid adsorption and dechlorination of 2,4-dichlorophenol. Materials Today Communication, 35:105983.

Hu, R., Cui, X., Xiao, M., Gwenzi, W. & Noubactep, C. (2020). Characterizing the impact of pyrite addition on the efficiency of $Fe^0/H_2O$ systems. Scientific Reports, 11: 2326.

Hussam, A. (2009). Contending with a Development Disaster: SONO Filters Remove Arsenic from Well Water in Bangladesh. Innovations 4:89–102.

Hussam, A. & Munir, A.K.M. (2007). A simple and effective arsenic filter based on composite iron matrix: Development and deployment studies for ground water of Bangladesh. Journal of Environmental Science and Health Part A, 42:1869-1878.

Jeen, S.W., Blowes, D.W. & Gillham, R.W. (2008). Performance evaluation of granular iron for removing hexavalent chromium under different geochemical conditions. Journal of Contaminant Hydrology, 95:76–91.

Kamolpornwijit, W., Liang, L.Y., West, O.R., Moline, G.R. & Sullivan, A.B. (2003). Preferential flow path development and its influence on long-term PRB performance: Column study. Journal of Contaminant Hydrology 66:161–178.

Kamolpornwijit, W. & Liang, L. (2006). Investigation of gas production and entrapmentin granular iron medium. Journal of Contaminant Hydrology, 82:338–356.

Kaur, P., Kumar, A., Babu, J.N. & Kumar, S. (2023). Tetracycline removal via three-way synergy between-pistachio shell powder, zerovalent copper or iron, and peroxymonosulfate activation. Journal of Hazardous Materials Advances, 12: 100385.

Li, D., Wen, Q.X. & Chen, Z.Q. (2024). Electric field coupled with $Fe_3O_4$ modified biochar to enhance anaerobic degradation of phenolic compounds in coal gasification wastewater (CGW). Separation and Purification Technology, 342:126950

Luo, P., Bailey, E.H. & Mooney, S.J. (2013). Quantification of changes in zero valent iron morphology using X-ray computed tomography. Journal of Environmental Sciences, 25: 2344–2351.

Mackenzie, P.D., Horney, D.P. & Sivavec, M.T. (1999). Mineral precipitation and porosity losses in granular iron columns. Journal of Hazardous Materials, 68:1–17.

Macêdo-Júnior, R. O., Campos, W. K., Buarque, F. S., Serpa, F. S., Silva, G. F., Santos, B. L., et al. & Ruzene, D. S. (2023). Utilization of corncob as adsorbent to remove oil and grease from produced water. Petroleum Science and Technology, 41(4): 477-492.

Miyajima, K. (2012). Optimizing the design of metallic iron filters for water treatment, Freiberg Online Geoscience 32: 60.

Ndé-Tchoupé, A.I., Hu, R., Gwenzi, W., Nassi, A. & Noubactep, C. (2020). Characterizing the reactivity of metallic iron for water treatment: $H_2$ evolution in $H_2SO_4$ and uranium removal efficiency. Water, 12, 1523.

Nitzsche, K. S., Lan, V.M., Kim, T.P.T., Viet, P.H., Berg, M., Voegelin, A., Planer- Friedrich, B., Zahoransky. J., Müller, S.K., Byrne, J.M., Schröder, C., Behrens, S. & Kappler, A. (2015). Arsenic removal from drinking water by a household sand filter in Vietnam—Effect of filter usage practices on arsenic removal efficiency and microbiological water quality. Science of the Total Environment, 502:526–536.

Njaramba, L.K., Park, J.-B., Lee, C.-S., Nzioka, A.M. & Kim, Y.-J. (2021). Permeable reactive barriers with zero-valent iron and pumice for remediation of groundwater contaminated with multiple heavy metals. Environment Engineering Science, 38: 245–255.

Noubactep, C. (2009a). Characterizing the effects of shaking intensity on the kinetics of metallic iron dissolution in EDTA, Journal Hazard Material, 170:1149–1155.

Noubactep, C. & Caré, S. (2010). Enhancing sustainability of household water filters by mixing metallic iron with porous materials. Chemical Engineering Journal, 162:635–642.

Noubactep, C. & Caré, S. (2011). Designing laboratory metallic iron columns for better result comparability. Journal Hazardous Materials, 189:809–813.

Noubactep, C. (2014). Flaws in the design of Fe (0)-based filtration systems. Chemosphere, 117:104–107.

Noubactep, C. (2015a). Designing metallic iron packed-beds for water treatment: A critical review. Clean-Soil, Air, 44:411-421.

Noubactep, C. (2015b). No scientific debate in the zero-valent iron literature. Clean-Soil, Air, Water. 44:330-332.

Ogata, R., Dangol, B., & Sakamoto, M. (2021). Sustainability assessment of long-term, widely used household Kanchan Arsenic Filters in Nepal. Journal of Environmental Science Health Part a Toxic Hazardous Substances and Environmental Engineering, 55: 517–527.

UNESCO (2021). *UN World Water Development Report 2021: Valuing Water*. Paris, France: UNESCO.

Rahman, M. A., Karmakar, S., Salama, H., Gactha-Bandjun., N, Btatkeu, K.B.D., Togué-Kamga, F., Btatkeu, K.B.D., Noubactep, C. & Woafo, P. (2011). Metallic Iron For Environmental Remediation: Back To Textbooks. Fresenius Environmental Bulletin, 21(7):1039–1044.

Senem, Y.G., Oruc, K.T., Emine, C.G., Narmin, G. & Gamze, V. (2023). Norfloxacin removal by ultraviolet-activated sodium percarbonate and sodium hypochlorite: process optimization and anion effect. Water Science & Technology, 87:2872-2889.

Shah, S. S., Sharma, T., Dar, B. A. & Bamezai, R. K. (2021). Adsorptive removal of methyl orange dye from aqueous solution using populous leaves: Insights from kinetics, thermodynamics and computational studies. Environmental Chemistry and Ecotoxicology, 3: 172-181.

Sorayyaei, S., Raji, F., Rahbar-Kelishami, A. & Ashrafizadeh, S.N. (2021). Combination of electrocoagulation and adsorption processes to remove methyl orange from aqueous solution. Environmental Technology & Innovation, 24(11): 102018.

Sun, J., Tian, A., Feng, Z., Zhang, Y., Jiang, F. & Tang, Q. (2021). Evaluation of zero-valent iron for Pb(II) contaminated soil remediation: From the analysis of experimental mechanism hybird with carbon emission assessment. Sustainability, 13, 452.

Tariq, J.A., Murat, Y., Amir, H. M., Samaneh, M. & Davoud, B. (2021). Ultraviolet radiation/persulphate/hydrogen peroxide treatment system for acid blue 80 dye degradation of batch flow chemical reactor: Effects of operational parameters, mineralisation, energy consumption, and kinetic studies. Research square, 04, 12-21. https://doi.org/10.21203/rs.3.rs-1071698/v1

Tepong-Tsindé, R., Crane, R., Noubactep, C., Nassi, A. & Ruppert, H. (2015a). Testing metallic iron filtration systems for decentralized water treatment at pilot scale. Water, 7:868–897.

Tepong-Tsindé, R., Phukan, M., Nassi, A., Noubactep, C. & Ruppert, H. (2015b). Validating the efficiency of the MB discoloration method for the characterization of $Fe^0/H_2O$ systems using accelerated corrosion by chloride ions. Chemical Engineering Journal, 279:353-362.

Togue-Kamga, F., Btatkeu, B.D., Noubactep, C., Woafo, P. (2012). Metallic iron for environmental remediation: Back to textbooks. Fresenius Environmental Bulletin, 21:1992–1997.

Xiao, M., Hu, R., Cui, X., Gwenzi, W. & Noubactep, C. (2020). Understanding the operating mode of $Fe^0$/Fe-sulfide/$H_2O$ systems for water treatment. Processes, 8, 409.

Yang, H., Hu, R., Ruppert, H. & Noubactep, C. (2021). Modeling porosity loss in $Fe^0$-based permeable reactive barriers with Faraday's law. Scientific Reports, 11, 16998.

Yang, H., Hu, R., Ndé-Tchoupé, A.I., Gwenzi, W., Ruppert, H. & Noubactep, C. (2020). Designing the next generation of $Fe^0$-based filters for decentralized safe drinking water treatment. Processes, 8, 745.

Yanne, E., Noubissié, E., Benessoubo, D. K., Eko, M. C. & Mbah, J. B. B. (2021). Physico-chemical study of the adsorption of methyl orange from water by biosorbent and activated carbon based on peanut shells. Journal of Energy, Environmental & Chemical Engineering, 6(2), 37-44.

Ying, S., Runan, G., Yaoxing, W., Xiaofei, D., Xueqi, L., Jianfu, T., Xuan, W., Jiuqing, L., Yanjun, X., Jian, L. & Wentao, G. (2023). Scalable Fabrication of Efficient and Recycling Wood Residue-Derived Sponge for Crude Oil Adsorption. Journal Of Hazardous Materials, 441(5): 129979.

You, Z., Osipov, Y., Bedrikovetsky, P. & Kuzmina, L. (2014). Asymptotic model for deep bed Filtration. Chemical Engineering Journal, 258:374–385.

Yuan, X., Y. Wang, P. Ji, P. Wu, J. Sheffield, & J. A. Otkin. (2023). "A Global Transition to Flash Droughts Under Climate Change." Science, 380: 187–191.

Zhang, Y., You, Q., Ullah, S., Chen, C., Shen, L. & Liu, Z. (2023). Substantial increase in abrupt shifts between drought and flood events in China based on observations and model simulations. Science of the Total Environment, 876: 162822.

Zhang, W., Wang, C.B. & Lien, H.L. (1998). Treatment of chlorinated organic contaminants with nanoscale bimetallic particles. Catalysis Today, 40: 387–395.

WHO/UNICEFF (2019). Progress on household drinking water, sanitation and hygiene 2000-2017 update.

WHO/UNICEFF (2025). Rapport mondial des Nations Unies sur la mise en valeur des ressources en eau 2025 Montagnes et Glaciers : des châteaux d'eau.

Zielina, M. (2011). Particle shapes in the drinking water filtration process. Clean: Soil Air, Water, 39: 941–946.